JOURNAL OF GUIDANCE, CONTROL, AND DYNAMICS
Vol. 21, No. 1, January–February 1998

Integrated Adaptive Control of Space Manipulators

L. Ehrenwald* and M. Guelman†
Technion—Israel Institute of Technology, Haifa 32000, Israel

Indirect adaptive control of space robot manipulators when maneuvering payloads with imperfectly known mechanical parameters is considered. The objective is to estimate system mechanical parameters during the maneuver itself. The system bodies are rigid and are concatenated by ideal, rotational joints. A new adaptive control law is developed that is applicable to general, rigid, multibody systems. It is based on the reinterpretation of the system dynamic equations as a measurement equation. The adaptive control law is of the integrated type; that is, the estimator part is used to estimate the integrated influence of the system mechanical parameters rather than the parameters themselves. The system equations of motion, control, and estimation are presented, and a formal solution is given. The parameter estimation process and the control law are analyzed separately. For constant generalized parameters, it is shown that the control-system output error is globally asymptotically stable and that the parameter error also will converge to zero if the external command input satisfies a certain sufficient excitation condition. A numerical simulation of a planar free-floating spacecraft with a two-degree-of-freedom robotic arm handling various payloads is presented.

I. Introduction

ALONG with the rapid development of the space industry during the last few decades, the need to lessen the actual human participation in space systems in order to save human efforts and avoid hazards has become clear. Autonomous robotic systems are about to become part of reality in space missions. Considerable research has been directed to some primary functions of robots in space applications,[1–7] as well as to the related technical issues such as kinematics, dynamics, and control.[7–26]

Robot manipulators carrying out extravehicular operations in space typically handle payloads with imperfectly known mechanical properties. Manipulator parameter and structural uncertainties, inaccuracies, modeled and unmodeled disturbances, and various couplings and nonlinearities not included in the model also appear in real tasks. Online estimation of those parameters and signals improves the quality of the maneuvers. To achieve this objective, recourse is taken to indirect adaptive control, i.e., the system parameters used in the control law are adjusted online, during execution of the desired maneuver.

Analyzing and simulating the existing manipulator (indirect) adaptive control methods[27–41] showed that, even for the simplest case of a one-link configuration, a number of algorithmical and numerical problems are still open.[42] When one considers generalization to the multilink case, these problems become even harder, and many more analytical, algorithmical, computational, and numerical ones appear. The most critical is probably the determination of the regressor matrix, a task too demanding for high-order systems such as a multiarmed space robot.

To avoid the need to generate the regressor matrix, a new adaptive control algorithm, the Integrated Adaptive Control, has been presented[42] to control multibody space robots. The algorithm is basically an indirect adaptive control method, in which the novelty is in the adaptive parameters definition. The generalized parameter matrices and vectors, which represent the integrated, time-varying effect of all unknown as well as supposedly known parameters, are directly estimated and tracked, rather than the basic mechanical parameters themselves as in all existing algorithms. This is achieved by reinterpreting the system dynamic equation as a linear time-varying measurement equation, in which those generalized parameters are time-varying parameters or state variables to be estimated. The generalized parameters vary slowly with time as applicable in the case of space manipulator operations. In the estimation scheme, the new parameters or state variables can be modeled as constants, deterministic time-varying, or stochastic. Once this viewpoint is adopted, known parameter or state estimation techniques[43,44] can be applied directly to this case. The controller part is of the certainty-equivalence type. The control law itself typically is the computed torque, either in joint space or in operational space.

The overall result is expected to be a more practical and general adaptive control algorithm. Because it effectively accounts for the integrated contribution of the unknown parameters to the generalized parameters, the regressor matrix needed in existing algorithms need never be formed here, which renders the proposed algorithm applicable to general multilink space manipulators. In addition, a rough convergence-rate analysis with comparison to existing schemes shows that, because the adaptive law and the control law are independently defined, the response is expected to be generally faster, smoother, and more uniform. The selection and tuning of numerical values for the parameters in the control and estimation parts of the scheme are more straightforward, too.

We generalize the theory and prove stability characteristics of the Integrated Adaptive Control, as well as present simulation results to demonstrate the potential performance of this algorithm in theory and in practice.

II. Space Manipulator Dynamics and Adaptive Control

We consider the space system as consisting of a rigid spacecraft to which the robot manipulator with one or two arms with several rigid links each is attached. For such a system, it can be shown that the overall equations of motion take the form[21,22,26]

$$H(\boldsymbol{q},\boldsymbol{p})\ddot{\boldsymbol{q}} + \boldsymbol{V}(\boldsymbol{q},\dot{\boldsymbol{q}},\boldsymbol{p}) = \boldsymbol{u} \tag{1}$$

where $\boldsymbol{q}$ is the vector of coordinates [degrees of freedom (DOF)], H is the generalized inertia matrix, $\boldsymbol{V}$ is the Coriolis load vector, $\boldsymbol{p}$ is the vector containing the mechanical system parameters, and $\boldsymbol{u}$ is the vector of applied forces and torques (associated with $\boldsymbol{q}$). Other effects such as gravity, friction, and various disturbances and uncertainties as mentioned in the Introduction, generally can be included in $\boldsymbol{V}$.

The control problem is to select the inputs $\boldsymbol{u}$ such that the coordinates $\boldsymbol{q}(t)$ track the desired time-varying coordinates $\boldsymbol{q}_d(t)$ with prescribed error dynamics $e(t)$, where

$$e(t) = \boldsymbol{q}(t) - \boldsymbol{q}_d(t) \tag{2}$$

When applying some form of the computed-torque approach for robotics manipulator control, either in joint space or in operational space, knowledge is required on the inertia matrix H and the Coriolis

Received Aug. 12, 1996; revision received July 10, 1997; accepted for publication July 25, 1997.

*Graduate Student, Faculty of Aerospace Engineering.

†Professor, Faculty of Aerospace Engineering.

vector $\boldsymbol{V}$. If the mechanical parameters vector $\boldsymbol{p}$ is unknown, except for some loose bounds, the matrix H and the vector $\boldsymbol{V}$ will not be computed correctly, and system performance can be degraded severely. This requirement for prior knowledge on the system mechanical parameters becomes even more acute for space robotic systems required to operate autonomously. The robotic manipulator is to be able to handle different payloads with unknown mass characteristics, and to operate in an unknown ambiance, hence the strong need for a technique for online estimation of the system parameters.

From a survey of the literature on adaptive control of manipulators,[27–41] including the detailed tutorials in Refs. 39 and 40, one can identify three approaches to adaptive control of robot manipulators. The first approach, Ref. 41, for example, developed during the early 1980s, is generally based on adaptive methods for linear time-invariant systems. For a multibody space manipulator to carry out the tasks described above, this is an unrealistic approach.[39] In the late 1980s, manipulator adaptive control algorithms that guarantee global stability appeared. They usually exploit the fact that the dynamic equations of a robot manipulator are linear in the parameters. These equations are parameterized so that the system dynamics are expressed as the product of a time-varying regressor matrix, supposedly available to the controller, and a constant unknown parameter vector to be estimated. This class of algorithms can be divided further into two groups: inverse-dynamics-based control (computed torque control) laws and passivity-based control laws. The first group[27,29–33] is based on global linearization and decoupling of the system equations, thus enabling the application of classical closed-loop linear control to get an exponentially stable system with prescribed error dynamics after adaptation. The second group[28,34–38] exploits the skew symmetry property (the Hamiltonian structure[40]) in the dynamic equations of a rigid manipulator in order to preserve the passivity property of the system in the closed loop. These algorithms do not lead to a closed-loop linear system, but possess some advantages, e.g., no need of joint acceleration measurements.

The mathematical outline of the main idea is as follows. The dynamics equation (1) is rewritten in the form

$$H(\boldsymbol{q},\boldsymbol{p})\ddot{\boldsymbol{q}} + \boldsymbol{V}(\boldsymbol{q},\dot{\boldsymbol{q}},\boldsymbol{p}) = Y(\boldsymbol{q},\dot{\boldsymbol{q}},\ddot{\boldsymbol{q}})\boldsymbol{p} = \boldsymbol{u} \tag{3}$$

where Y is a matrix of known structure that depends on known kinematic quantities. It is referred to as the regressor matrix. The vector $\boldsymbol{p}$ contains the system mechanical parameters that are to be estimated.[27,28,39] Assume, without loss of generality, that the control law is based on the proportional-plus-derivative (PD) computed torque type in joint space,

$$\boldsymbol{u} = \bar{H}(\ddot{\boldsymbol{q}}_d - k_v\dot{\boldsymbol{e}} - k_p\boldsymbol{e}) + \bar{\boldsymbol{V}} \tag{4}$$

where $\bar{H}$ and $\bar{\boldsymbol{V}}$ represent estimates of H and $\boldsymbol{V}$, respectively, based on the estimate $\bar{\boldsymbol{p}}$ of $\boldsymbol{p}$ and the supposedly known parameters. With this control law, one derives

$$\ddot{\boldsymbol{e}} + k_v\dot{\boldsymbol{e}} + k_p\boldsymbol{e} = \bar{H}^{-1}Y(\bar{\boldsymbol{p}} - \boldsymbol{p}) \tag{5}$$

Then, one chooses a parameter-estimate update law, typically of the type

$$\dot{\bar{\boldsymbol{p}}} = \boldsymbol{f}(\boldsymbol{e}, \dot{\boldsymbol{e}}, \boldsymbol{y}) \tag{6}$$

The choice of the update law is made in general such that a specified Lyapunov function fulfills the requirements to prove global stability for the output error $\boldsymbol{e}$. If the system inputs are persistently exciting, one can show in addition the global asymptotic stability of the parameter estimation error $\bar{\boldsymbol{p}} - \boldsymbol{p}$.[27,28,39]

In Ref. 42, use of this approach for the single-axis motion of a rigid body was analyzed and numerically simulated. Five representative existing algorithms[27–31] were investigated, and two of them[27,28] were selected for numerical evaluation. Generally, the results showed that even in this simplest case a number of drawbacks appear in existing algorithms. When one considers the general, multilink case, these problems become even more severe and many more problems—algorithmical, numerical, analytical, and computational—are to be resolved. The literature shows applications to rather simple configurations, with two or, at most, three DOF. For the case of a representative multilink space manipulator attached to a spacecraft, no simulation results could be found in the literature scanned. The most obvious explanation for this fact could well be that the construction of the regressor matrix (preparatory to the definition of the adaptive control law) is too demanding for a high-order system. Moreover, the application of passivity-based algorithms to a space-based manipulator is feasible only when the base (the spacecraft) is orientation controlled[34,36]; otherwise, there is no passivity. This renders the whole group of passivity-based adaptive algorithms inapplicable to the important case of a free-floating system. This analysis motivated the introduction of the Integrated Adaptive Control method. We now review the Integrated Adaptive Control.

III. Integrated Adaptive Control

In most of the existing manipulator adaptive control algorithms, the vector $\ddot{\boldsymbol{q}}$ of coordinate accelerations was considered to be part of the measured variables. Once this viewpoint is adopted for the joint accelerations, the system dynamics equation (1) can be seen in a new light. Equation (1) becomes a linear time-varying measurement equation, where now the generalized inertia matrix elements as well as the Coriolis-vector components can be regarded as the parameters or states to be estimated and where the vector of commanded torques $\boldsymbol{u}$ defines a time-varying measurement matrix, as now shown.

System equation (1) can be inverted (because the mass matrix has the property $H = H^T > 0$) to obtain

$$\ddot{\boldsymbol{q}} = H^{-1}\boldsymbol{u} - H^{-1}\boldsymbol{V} \tag{7}$$

Define

$$M = H^{-1} = \left[\mathrm{row}\left(\boldsymbol{m}_i^T\right)\right], \qquad i = 1, 2, \ldots, n \tag{8}$$

and

$$\boldsymbol{b} = -H^{-1}\boldsymbol{V} \tag{9}$$

Hence,

$$H^{-1}\boldsymbol{u} = \begin{bmatrix} \boldsymbol{m}_1^T \\ \vdots \\ \boldsymbol{m}_n^T \end{bmatrix}\boldsymbol{u} = U\boldsymbol{m} \tag{10}$$

where

$$U = \begin{bmatrix} \boldsymbol{u}^T & & \\ & \ddots & \\ & & \boldsymbol{u}^T \end{bmatrix}, \qquad \boldsymbol{m} = \begin{bmatrix} \boldsymbol{m}_1 \\ \vdots \\ \boldsymbol{m}_n \end{bmatrix} \tag{11}$$

with $\dim U = n \times n^2$ and $\dim \boldsymbol{m} = n^2$. Equation (7) then reads

$$z(t) = C\boldsymbol{x}(t) \tag{12}$$

where

$$z = \ddot{\boldsymbol{q}}, \qquad \boldsymbol{x} = \begin{bmatrix} \boldsymbol{m} \\ \boldsymbol{b} \end{bmatrix}, \qquad C = [U, I_{n\times n}] \tag{13}$$

with $\dim z = n$, $\dim \boldsymbol{x} = n^2 + n$, and $\dim C = n \times (n^2 + n)$. The vector z consists of measurements of accelerations. The time-varying matrix C consists of the commanded control inputs as generated by the control system. The parameter or state vector $\boldsymbol{x}$ consists of unknown elements of the inverse mass matrix and of the weighted Coriolis vector.

The estimation model, i.e., the system equation for parameter or state estimation, the measurement equation, and the estimation algorithm now can be defined on the basis of estimation theory. The simplest procedure is to regard the unknown parameter vector $\boldsymbol{x}$ as constant, i.e., $\dot{\boldsymbol{x}} = 0$, and the measurements as given by Eq. (12) and to choose a continuous-time linear recursive estimator,

$$\dot{\bar{\boldsymbol{x}}} = K(t)(z - C\bar{\boldsymbol{x}}) \tag{14}$$

the most efficient of which is the recursive least-squares (RLS) algorithm, where

$$K = PC^T \tag{15}$$

and

$$\dot{P} = -PC^T CP \tag{16}$$

with initial conditions

$$\boldsymbol{x}(0),\ P(0) = k_0 I > 0 \tag{17}$$

From the estimate $\bar{\boldsymbol{x}}$ of $\boldsymbol{x}$, one obtains estimates of the inverse mass matrix $\bar{M}$ and of the weighted Coriolis vector $\boldsymbol{b}$. From these, one obtains $\bar{H}$ and $\bar{V}$ as desired. The latter data are inserted in the control law.

Because in the actual system the generalized parameters are time-varying, covariance resetting[44,45] is implemented to render the estimator capable of tracking time-varying parameters. This means resetting the matrix P according to

$$P\left(t_r^+\right) = P(0) \tag{18}$$

where

$$t_r \in \{t_1, t_2, t_3, \ldots\}$$

The procedure suggested in Eqs. (7–18) involves high-order matrices and so might be computationally demanding. In practice, however, there is no need to use these equations. Because U is block-diagonal with repetitive $\boldsymbol{u}^T$, Eq. (12) actually consists of a set of independent equations,

$$z_i = [\boldsymbol{u}^I, 1]\begin{pmatrix}\boldsymbol{m}_i\\ b_i\end{pmatrix} = \boldsymbol{c}^T\boldsymbol{x}_i, \qquad i = 1, 2, \ldots, n \tag{19}$$

and so the process in Eqs. (14–18) can be accomplished by n parallel ones:

$$\dot{\bar{\boldsymbol{x}}}_i = k_i(t)\left(z_i - \boldsymbol{c}^T\bar{\boldsymbol{x}}_i\right) \tag{20}$$

where

$$k_i = p_i\boldsymbol{c} \tag{21}$$

and

$$\dot{p} = -p\boldsymbol{c}\boldsymbol{c}^T p \tag{22}$$

Here dim $z_i = 1$, dim $\boldsymbol{x}_i = n+1$, dim $\boldsymbol{c}^T = 1 \times (n+1)$, and dim $p = (n+1)\times(n+1)$. The only unavoidable relatively heavy computation is the inversion of the estimate $\bar{M}$, where dim $\bar{M} = n \times n$, to get $\bar{H}$.

Note that the outlined process does not estimate the unknown parameter vector $\boldsymbol{p}$ appearing in other adaptive control techniques. Instead, it estimates effectively only the elements of the inverse mass matrix and the components of the weighted Coriolis vector. This is then a form of integrated adaptive control. For large-scale systems, it has the considerable advantage that one does not need to derive explicit expressions for the mass matrix, the Coriolis vector, and the regressor matrix. The new technique simply produces the final result. At the same time, the problem of defining a parameter vector $\boldsymbol{p}$, containing observable parameters only, has been avoided at the expense of tracking the time variation of the generalized parameters. The effects of any time variations in the mechanical parameters themselves therefore are tracked also.

The control law itself has yet to be introduced. The control law specifies the vector $\boldsymbol{u}$ that enters into the measurement matrix C. The selection of the control law therefore also influences the estimator, as expected. Indeed the requirement of persistent excitation, mentioned in Sec. II, surfaces here again, albeit in a different form, as shown in Sec. IV.

The control law may be in the form of the usual joint space computed torque control type, mentioned in Sec. II. It also may be in the form of the operational-space (or Cartesian) control type, where the end-effector position and orientation are controlled directly.[21,22,26,42]

It is difficult to rigorously analyze the performance of an adaptive control system with time-varying parameters. One highly desirable property is, however, that the algorithm at least be globally convergent if the parameters are time invariant. In the next section, we show that this is actually the case in the Integrated Adaptive Control, if the computed torque control law is coupled with a linear recursive parameter estimator through the certainty equivalence principle.

IV. Output and Parameter Error

According to the explanation in the preceding paragraph, the stability analysis refers to the system equations after substitution for the special case of constant parameters. For simplicity, we refer to the joint space control [Eq. (4)], but the same conclusions hold for the operational space control.

Collecting and manipulating Eqs. (1), (4), and (14–16), defining the parameter error vector as

$$\boldsymbol{x}_e = \bar{\boldsymbol{x}} - \boldsymbol{x} \tag{23}$$

and taking $\dot{\boldsymbol{x}} = 0$ in Eq. (14) for constant parameters, we get the overall system dynamic equations in state-space form, i.e., $\dot{\boldsymbol{y}} = f(t, \boldsymbol{y})$,

$$\dot{\varepsilon} = A\varepsilon + g \tag{24}$$

$$\dot{x}_e = -Bx_e \tag{25}$$

$$\dot{P} = -BP \tag{26}$$

where

$$\varepsilon = \begin{bmatrix} e\\ \dot{e}\end{bmatrix} \tag{27}$$

$$A = \begin{bmatrix} 0 & I\\ -k_p I & -k_v I\end{bmatrix} \tag{28}$$

$$g = \begin{bmatrix} 0\\ -Cx_e\end{bmatrix} \tag{29}$$

$$B = PC^T C \tag{30}$$

$$u = \bar{M}^{-1}(\ddot{q}_d - [k_p I, k_v I]\varepsilon - \bar{b}) \tag{31}$$

and $\bar{M}$, $\bar{b}$ are the estimates of M, b, respectively, defined in Eqs. (8) and (9).

On the basis of regular (nonlinear) differential equations theory (specifically, uniqueness, existence, and extension theorems), one can show that under rather natural conditions on the desired trajectory [namely, $\ddot{\boldsymbol{q}}_d(t)$ is piecewise-continuous and bounded], all of the signals in the system are piecewise uniformly continuous and bounded, and a unique solution, $\boldsymbol{y}[\ddot{\boldsymbol{q}}_d(t)] = \boldsymbol{y}(t) = \boldsymbol{y}(t; \underline{0}, y_0)$, exists for $0 \le t < \infty$ and any physical initial state, i.e., $\bar{H}(0) > 0$, provided that the estimated inverse generalized inertia matrix is guaranteed to be positive definite and lower bounded, i.e., $\bar{H}^{-1} \equiv \bar{M} \ge \alpha I > 0$. In the single-axis case, this condition obviously exists by the definition of the scalar estimation equation. In the general, multi-DOF case, we assume that the condition holds. Otherwise, proper artificial bounds on the estimate $\bar{M}$ solve this problem adequately.

A direct closed formula for this solution does not exist. However, it is possible to represent the system solution as a direct function of $\boldsymbol{u}(t)$, which is the immediate input to both the controller and the estimation parts. Starting with Eq. (26), it can be verified that the solution is

$$P(t) = \left[P(0)^{-1} + \int_0^t C^T C\,\mathrm{d}t\right]^{-1} \tag{32}$$

Then, noting the similarity of Eqs. (25) and (26), the solution to Eq. (25) is

$$\boldsymbol{x}_e(t) = \left[P(0)^{-1} + \int_0^t C^T C\,\mathrm{d}t\right]^{-1} P(0)^{-1}\boldsymbol{x}_e(0) \tag{33}$$

The solution to Eq. (24) is, by the variation of parameters,

$$\varepsilon(t) = \varepsilon_h(t) + \int_0^t E(t-\alpha) g(\alpha)\,\mathrm{d}\alpha \tag{34}$$

where $\varepsilon_h(t)$ is the solution of $\dot{\varepsilon}_h = A\varepsilon_h$ with $\varepsilon_h(0) = \varepsilon(0)$ and $E(t)$ is the fundamental system of solutions of $\dot{E} = AE$ with $E(0) = I$.

A. Output-Error Convergence

Examining the estimation-error equation (25), it seems intuitively clear that either $\boldsymbol{x}_e$ or $C = [U, I]$, or some combination of both, should approach zero as $t \to \infty$.

To prove this mathematically, the following Lyapunov method is employed. Define the scalar function

$$V(\boldsymbol{x}_e, P) = \boldsymbol{x}_e^T P^{-1} \boldsymbol{x}_e \tag{35}$$

Because $P > 0$ for all t [from Eq. (26) or (32) because $P(0) > 0$ by definition of a covariance matrix], V is positive definite. The time derivative of V along the trajectories of $\boldsymbol{x}_e$ and P is

$$\dot{V}(\boldsymbol{x}_e, P) = -\boldsymbol{x}_e^T C^T C \boldsymbol{x}_e \tag{36}$$

which also takes the form

$$\dot{V} = -|C\boldsymbol{x}_e|^2 = -|v|^2 \tag{37}$$

Because $V > 0$ and $\dot{V} \le 0$, V is a nonnegative and monotonous nonincreasing function, and so, the limit $V(\infty)$ exists, and

$$|V(\infty) - V(0)| = \left| \int_0^\infty \dot{V}\,\mathrm{d}t \right| = \int_0^\infty |v|^2\,\mathrm{d}t < \infty \tag{38}$$

Also, because all signals in the system are (piecewise) uniformly continuous, v (and hence $|v|^2$) is also piecewise uniformly continuous. According to the lemma of Barbalat,[45] then, $\lim_{t\to\infty} |v| = 0$, which implies that $\lim_{t\to\infty} |C\boldsymbol{x}_e| = 0$. [The lemma says that, if $f : R^+ \to R$ is uniformly continuous for $t \ge 0$ and if the limit of the integral

$$\lim_{t\to\infty} \int_0^t |f(\tau)|\,\mathrm{d}\tau$$

exists and if finite, then $\lim_{t\to\infty} f(t) = 0$.] Thus, we get

$$\lim_{t\to\infty} C\boldsymbol{x}_e = 0 \tag{39}$$

Now, we turn our attention to the output-error equation (24). Given that A has been chosen asymptotically stable [Eq. (4)], $g(t)$ is a (piecewise) continuous function of t for $0 \le t < \infty$ and

$$\lim_{t\to\infty} \boldsymbol{g}(t) \equiv \lim_{t\to\infty} \begin{bmatrix} 0 \\ -C\boldsymbol{x}_e(t) \end{bmatrix} = 0$$

it follows then that

$$\lim_{t\to\infty} \varepsilon(t) = \boldsymbol{0} \tag{40}$$

B. Parameter-Error Convergence

Having concluded that $\lim_{t\to\infty} C\boldsymbol{x}_e = 0$ and $\lim_{t\to\infty} \varepsilon(t) = 0$, let us examine the parameter-error $\boldsymbol{x}_e$ convergence to zero as $t \to \infty$. The $\boldsymbol{x}_e$ convergence is dependent on the time behavior of $U(t)$, and therefore of $\boldsymbol{u}(t)$, through the so-called persistency of excitation (PE) condition, which now is developed for the relevant system.

From Eq. (33), it is clear that the necessary and sufficient condition for $\lim_{t\to\infty} \boldsymbol{x}_e(t) = 0$ is

$$\int_0^\infty C^T C\,\mathrm{d}t \equiv \int_0^\infty \begin{bmatrix} U^T \\ I \end{bmatrix} [U, I]\,\mathrm{d}t = \infty \tag{41}$$

However, the matrix $U^T U$ is of rank n, which indicates some redundancy in expression (41). Noting that

$$\begin{bmatrix} U^T \\ I \end{bmatrix} [U, I] = \left[\begin{array}{ccc|ccc} \boldsymbol{u}\boldsymbol{u}^T & & & \boldsymbol{u} & & \\ & \ddots & & & \ddots & \\ & & \boldsymbol{u}\boldsymbol{u}^T & & & \boldsymbol{u} \\ \hline \boldsymbol{u}^T & & & & & \\ & \ddots & & & I & \\ & & \boldsymbol{u}^T & & & \end{array}\right] \tag{42}$$

we conclude that expression (41) can be reduced to

$$\int_0^\infty \boldsymbol{u}(t)\boldsymbol{u}(t)^T\,\mathrm{d}t = \infty \tag{43}$$

From the applications point of view, we are interested in PE conditions on the external, independent, input vector $\ddot{\boldsymbol{q}}_d(t)$ rather than on the control vector $\boldsymbol{u}(t)$ generated by the controller. Because the output error converges to zero, independently of PE conditions, we can substitute $\lim_{t\to\infty} \varepsilon(t) = 0$ in Eq. (31) to get

$$\lim_{t\to\infty} \boldsymbol{u}(t) = \bar{H}\ddot{\boldsymbol{q}}_d(t) + \bar{\boldsymbol{V}} \equiv \bar{M}^{-1}[\ddot{\boldsymbol{q}}_d(t) - \bar{\boldsymbol{b}}] \tag{44}$$

Because we also know that $\bar{M}$ and $\bar{\boldsymbol{b}}$ are bounded and $\bar{M} \ge \alpha I > 0$, we conclude that Eq. (44) can be considered an algebraic transformation between the $\boldsymbol{u}(t)$ PE condition and the $\ddot{\boldsymbol{q}}_d(t)$ PE condition. Because the PE condition is invariant under algebraic transformations,[45] the PE condition on $\ddot{\boldsymbol{q}}_d(t)$ is

$$\int_0^\infty \ddot{\boldsymbol{q}}_d(t)\ddot{\boldsymbol{q}}_d(t)^T\,\mathrm{d}t = \infty \tag{45}$$

The parameter error vector converges to zero if and only if condition (45) is fulfilled.

V. Operational-Space Integrated Adaptive Control Torque for Space Manipulators

Applying the usual joint space control in the case of a free-flying robot might not be practical, because the manipulator-joint angles that normally would be commanded in the case of a fixed base will fail to achieve the required task because of the dynamic and kinematic interaction between the manipulator and the base. It seems natural, then, to apply operational-space control, i.e., the end effector will be controlled directly through the joint torques, to track a prescribed time-dependent trajectory, with no need to compute the joint trajectories preparatory to the control.

Although, in the operational-space approach, the end effector is directly controlled, the actual measured states of the system are the joint angles and rates and the driven elements are the joint torques. In consequence, it is in terms of these variables that the system equations are considered.

As with joint-space computed torque control, the knowledge of the generalized inertia matrix and the Coriolis vector of the manipulator also is required for the correct application of operational-space computed torque control, and thus those generalized parameters should be estimated when some or all of the mechanical parameters are unknown. Furthermore, without repeating the proof details, all previous results developed specifically for the case of joint-space control of a spacecraft–manipulator system are immediately applicable or naturally generalizable to operational-space control of a manipulator on a free-floating spacecraft.

Following the development in Refs. 22 and 26, one first transforms the dynamic model for the entire spacecraft–manipulator system into an effective dynamic model for the manipulator only. The resulting equation takes the general form of Eq. (1), with an appropriately modified interpretation of the terms involved:

$$H_m \ddot{\boldsymbol{q}}_m + \boldsymbol{V}_m = \boldsymbol{u}_m \tag{46}$$

The relation between the end-effector (linear) velocity, the robot joint rates, and the spacecraft linear and angular velocity is defined by

$$\dot{x} = J_s\dot{x}_s + J_m\dot{q}_m = J\nu \tag{47}$$

where $\nu = [\dot{x}_S^T, \dot{q}_m^T]^T$ is the combined vector of spacecraft and joint velocities, $\dot{x}$ is the end-effector velocity vector, and $J = [J_s, J_m]$ is the (augmented) Jacobian matrix. Differentiation of the last expression with respect to time gives the acceleration relation

$$\ddot{X} = \dot{J}_s\dot{x}_s + J_s\ddot{X}_s + \dot{J}_m\dot{q}_m + J_m\ddot{q}_m \tag{48}$$

For the end effector to be controlled directly by the joint torquers so that a commanded acceleration $\ddot{X}_c$ is attained, the commanded joint acceleration therefore should be

$$\ddot{q}_m = J_m^{-1}(\ddot{X}_c - \dot{J}_s\dot{x}_s - J_s\ddot{X}_s - \dot{J}_m\dot{q}_m) \tag{49}$$

where $\ddot{X}_c$ may be defined by any control function assuring the required response for each one of the end-effector state components, for example, the PD controller,

$$\ddot{X}_c = \ddot{X}_d - k_v\dot{e} - k_p e, \qquad e = X - X_d \tag{50}$$

Substituting Eq. (49) into Eq. (46), the joint control torque is finely defined as

$$u_m = \bar{H}_m J_m^{-1}(\ddot{X}_c - \dot{J}_s\ddot{X}_s - J_s\ddot{X}_s - \dot{J}_m\dot{q}_m) + \bar{V}_m \tag{51}$$

where now $\bar{H}_m$ and $\bar{V}_m$ are the estimated values of H_m and V_m, respectively; q_m, $\dot{q}_m$, and $\dot{x}_s$ are measured; J_s and J_m are computed on the basis of $\dot{q}_m$ and the assumed known geometric properties of the manipulator; and $\ddot{X}_s$ could either be measured or computed, based on the reaction force and torque exerted by the manipulator on the spacecraft.

Figure 1 depicts a general block diagram of the operational-space computed torque control system.

VI. Numerical Examples

Simulations were carried out to show the feasibility of the Integrated Adaptive Control when the estimated parameters are time varying as in the real case.

The operational-space control of a free-floating (i.e., no controls are applied to the spacecraft) planar space robot with a two-link manipulator was considered. The robotic arm has two rotational DOF, being thus able to control the end-effector position in the plane. The spacecraft itself adds another three DOF.

This free-floating robot is to be able to handle payloads with large variations in mass properties. The control system should be able to adapt itself to these varying conditions. This was the essential motivation behind the development of this integrated adaptation.

The assumed known mass properties of this space robot are given in Table 1, where for each body the moment of inertia is given with respect to the body center of mass. The initial conditions for the joint angles for all simulations to be considered here are given in Table 2. For these given initial conditions, the end effector is at rest at initial time. The operational-space control law used the values $k_p = 4$ and $k_v = 4$ for each of the two end-effector controlled coordinates. The changes in payload mass properties were introduced by adding a point mass of different sizes to the end-effector.

Two experiments are considered. The purpose of the first one is to demonstrate the ability of the Integrated Adaptive Control to make the end-effector precisely track a complex time-dependent trajectory when the actual payload is very heavy relative to the assumed one. The purpose of the second experiment is to show how the Integrated Adaptive Control stabilizes the response of the end-effector when the payload is unexpectedly dropped.

In both examples, the desired end-effector task is to transfer a payload from given initial conditions to prespecified final conditions in a given time, along a specific path. The planned trajectory is a linear interpolation with a trapezoidal velocity profile, including a half-circle trajectory encircling an assumed obstacle, as shown in Fig. 2. The constant demanded velocity along the circle is proportionally higher, and so, a velocity step input is created. The requirement to complete this trajectory in a given time was included to represent the case of rendezvous with a second vehicle.

Table 1 Space robot parameter values

	Length, m	Mass, kg	Moment of inertia, kg · m^2
Spacecraft	1	500	41.5
Manipulator links	2	25	8.3

Table 2 Space robot initial conditions

Joint angles	$q_{m1}(0) = 0$, $q_{m2}(0) = 2\pi/3$
Joint angle rates	$\dot{q}_{m1}(0) = 0$, $\dot{q}_{m2}(0) = 0$
Spacecraft position and attitude	**0**
Spacecraft velocity and rate	**0**

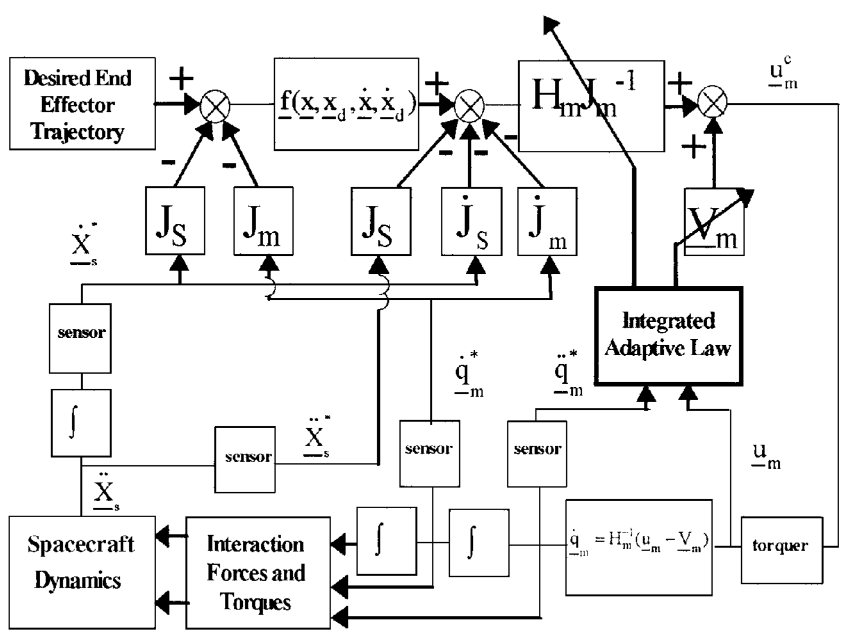

Fig. 1 Block diagram of operational-space manipulator Integrated Adaptive Control for a free-floating spacecraft.

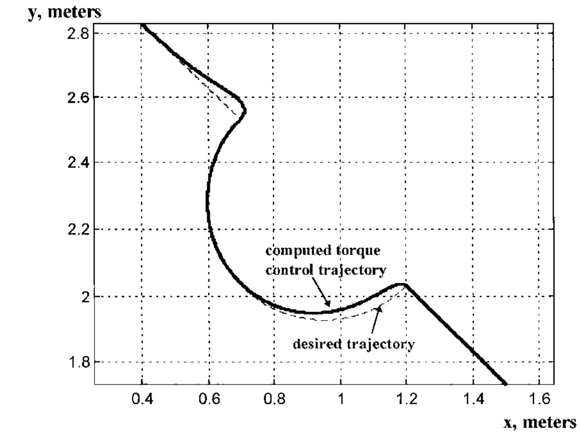

Fig. 2 End effector desired and computed torque trajectory with perfectly known system parameters.

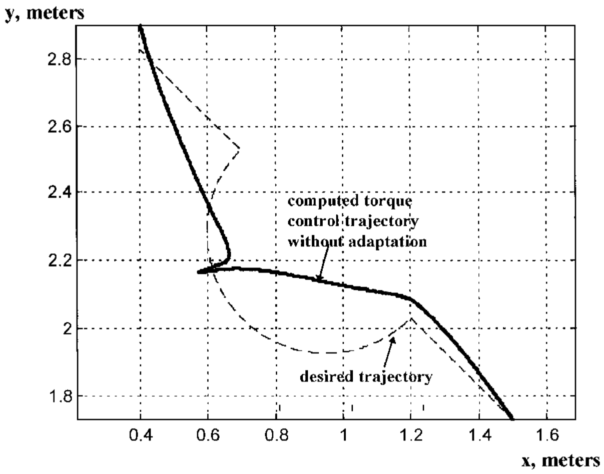

Fig. 3 End-effector trajectory with unknown payload for control system and no adaptation.

First, a simulation without the payload is performed; that is, nominal system parameters were employed and known to the control system. The actual evolution of the end-effector position is shown in the same Fig. 2. As expected, the system behavior is the ideal velocity PD control response.

Next, a relatively large payload (200 kg) is attached to the end effector. The control law without adaptation uses the same system parameters as previously. This implies a mismatch between H_m and $\boldsymbol{V}_m$ in the dynamic model and their values as used in the control law. As seen in Fig. 3, the system performance is strongly degraded, convergence is slow, and, in the present example, this would mean a collision with the obstacle.

The Integrated Adaptive Control law then is implemented. Figure 4 shows the end-effector trajectory with the Integrated Adaptive Control implemented with the initial estimates for the generalized inertia matrix and Coriolis vector computed, according to the nominal (wrong) system parameters. The numerical values of the estimation algorithm are $k_0 = 50$, $t_r \in \{0.1\text{ s}, 0.2\text{ s}, 0.3\text{ s}, \ldots\}$. As can be seen, the performance is virtually equal to the ideal performance in spite the incorrect initial values of the generalized inertia matrix and Coriolis vector, the presence of the unknown payload, and the fact that the system parameters are time varying.

Additional runs were performed with the Integrated Adaptive Control; the initial estimates for the generalized inertia matrix and the Coriolis vector were arbitrarily chosen to be the identity matrix and the zero vector, respectively. Results were still practically equal to the ideal performance.

To get a better understanding of the system behavior with the Integrated Adaptive Control it is constructive to observe the behavior of the driving function g of the output-error vector ε as defined in Eq. (24). The time behavior of the components of the matrix product $\boldsymbol{C}\boldsymbol{x}_e$, which constitute the nonzero components of the driving

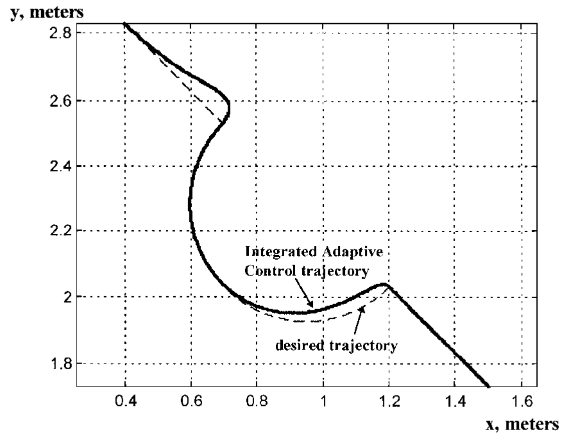

Fig. 4 End-effector trajectory with unknown payload for control system and integrated adaptative control.

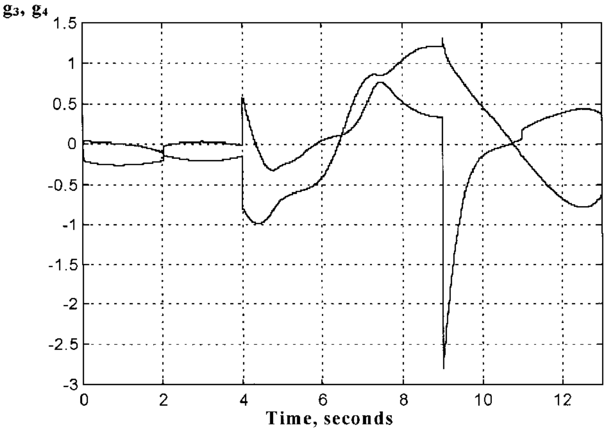

Fig. 5 Output-error driving-function components for the case of unknown payload and no adaptation.

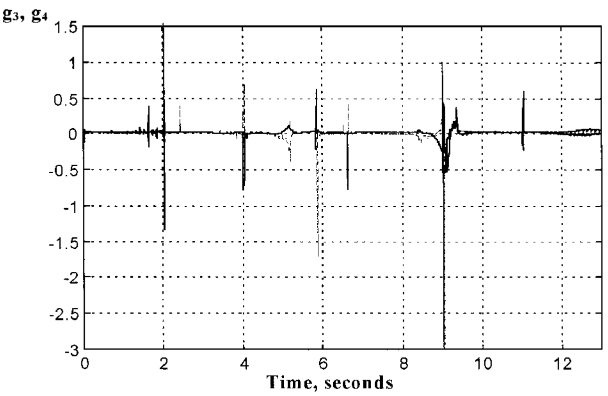

Fig. 6 Output-error driving-function components for the case of Integrated Adaptive Control.

function g as defined in Eq. (29), for both the case of no adaptation and that of integrated adaptation, is shown in Figs. 5 and 6, respectively. Without adaptation, the driving function does not converge to zero. Under the proposed adaptive algorithm, this signal is supposed to converge to zero with time, as the proof in Sec. IV.A indicates [Eq. (39)], thereby implying that the output error also converges to zero. This property is clearly evident in Fig. 6. The sharp peaks indicate the presence of jumps in the commanded acceleration, but convergence to zero is very fast, so that the average values of each of the two components of this vector are virtually zero on any finite time interval. This is the reason for the excellent control performance shown in Fig. 4.

In the second example, during the first half second of the motion, a known payload of 505 kg is attached to the end effector. Then, the

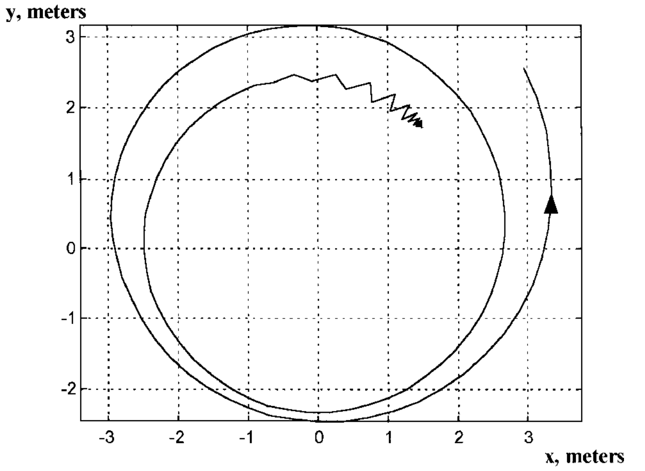

Fig. 7 End-effector trajectory when dropping the payload while in motion with no adaptation.

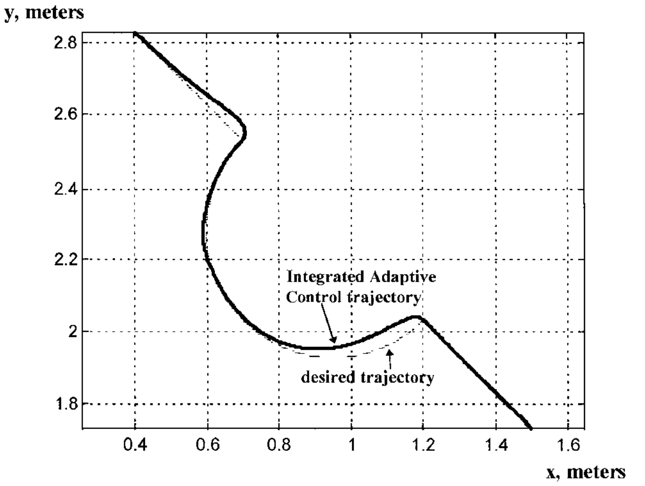

Fig. 8 Integrated Adaptive Control end-effector trajectory with unknown payload for the control system (payload is unexpectedly dropped while in motion).

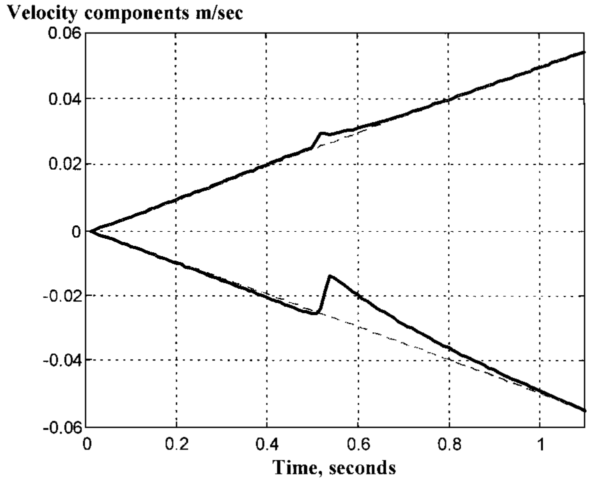

Fig. 9 Integrated Adaptive Control end-effector velocity convergence after dropping the payload.

end effector drops the payload but is expected to continue tracking the same desired trajectory.

If the actual system parameters are known to the control system for all t, before and after dropping the payload, the system behavior is the ideal velocity PD control response, resulting again, as expected, in the trajectory depicted in Fig. 2.

When the payload is dropped unexpectedly, the control system does not know that a change in system parameters has occurred and therefore continues to use the same ones as previously. The actual evolution of the end-effector position in this case is shown in Fig. 7. As clearly seen in Fig. 7, under the mismatch between actual and assumed parameters, the system becomes unstable.

A simulation of the same task using Integrated Adaptive Control then is implemented. As can be seen in Fig. 8, the system remains stable after the step change in parameters at $t = 0.5$ s, and performance is maintained in spite of the large mismatch in parameters.

Figure 9 shows the response of the end-effector velocity components to the step change in parameters caused by dropping the payload. There is a short transient disturbance at $t = 0.5$ s, after which the steady-state desired trajectory again is maintained.

VII. Conclusions

Attention is focused on adaptive control of space manipulators with rigid links and unknown mechanical parameters. To handle the large-scale control problems of space manipulators, the system dynamics equation is reinterpreted in terms of a linear, time-varying measurement equation. With this approach, the parameters to be estimated represent the integrated effect of all unknown as well as supposedly known parameters, as represented by the inverse mass matrix and the weighted Coriolis vector. This reinterpretation allows well-known estimation techniques to be applied directly to this case. This approach avoids the task of explicitly constructing the regressor matrix, as required by present adaptive control techniques.

The stability and convergence characteristics of the proposed adaptive control scheme are analyzed. It is proven that the output (tracking) error is globally asymptotically stable, and that if the system input (the desired trajectory) is persistently exciting, the generalized parameter error converges to zero as well.

The analytical stability and convergence results obtained here strictly apply for the case of constant generalized parameters. Actually, these parameters are slowly varying functions of time. Application of the Integrated Adaptive Control requires continuous tracking of the generalized-parameter time variations. To estimate and track the parameters with the RLS algorithm, the covariance matrix update is modified to prevent the gain matrix from approaching zero, thus guaranteeing exponential convergence.

Numerical simulations of a planar free-floating spacecraft with a two-DOF arm were performed. Applying computed torque control with an unknown payload attached to the end effector always resulted in poor system performance and it even became unstable for the case of payload dropping. On the other hand, when the Integrated Adaptive Control developed here is applied, the system behavior in all cases is very close to the ideal case.

References

[1]Whittaker, W. L., and Kanade, T., "Space Robotics in Japan," Loyola College, Baltimore, MD, 1991.

[2]Ullman, M., and Cannon, R., "Experiments in Global Navigation and Control of Free-Flying Space Robot," *Proceedings of the ASME Winter Annual Meeting*, American Society of Mechanical Engineers, New York, 1989, pp. 37–43.

[3]Xu, Y., and Kanade, T., *Space Robotics: Dynamics and Control*, Kluwer Academic, Boston, 1992.

[4]Becker, U., and Kerstein, L., "An Evolutionary Approach Towards Unmanned Orbital Servicing," *Space Technology*, Vol. 12, No. 1, 1992, pp. 45–56.

[5]Hirzinger, G., Brunner, B., Dietrich, J., and Heindl, J., "Sensor-Based Space Robotics—ROTEX and Its Telerobotic Features," *IEEE Transactions on Robotics and Automation*, Vol. 9, No. 5, 1993, pp. 649–663.

[6]Andary, J. F., and Spidaliere, P. D., "The Development Test Flight of the Flight Telerobotic Servicer: Design, Descriptions and Lessons Learned," *IEEE Transactions on Robotics and Automation*, Vol. 9, No. 5, 1993, pp. 664–674.

[7]Book, W. J., "Structural Flexibility of Motion Systems in the Space Environment," *IEEE Transactions on Robotics and Automation*, Vol. 9, No. 5, 1993, pp. 524–530.

[8]Dubowsky, S., and Papadopoulos, E., "The Kinematics, Dynamics, and Control of Free-Flying and Free-Floating Space Robotic Systems," *IEEE Transactions on Robotics and Automation*, Vol. 9, No. 5, 1993, pp. 531–543.

[9]Murphy, S. H., and Ting-Yung Wen, J., "Analysis of Active Manipulator Elements in Space Manipulation," *IEEE Transactions on Robotics and Automation*, Vol. 9, No. 5, 1993, pp. 544–552.

[10]Carusone, J., Buchan, K. S., and D'Eleuterio, G. M. T., "Experiments in End-Effector Tracking Control for Structurally Flexible Space Manipulators," *IEEE Transactions on Robotics and Automation*, Vol. 9, No. 5, 1993, pp. 553–560.

[11]Mukherjee, R., and Chen, D., "Control of Free-Flying Underactuated Space Manipulators to Equilibrium Manifolds," *IEEE Transactions on Robotics and Automation*, Vol. 9, No. 5, 1993, pp. 561–570.

[12]Yokokohji, Y., Toyoshima, T., and Yoshikawa, T., "Efficient Computational Algorithms for Trajectory Control of Free-Flying Space Robots with Multiple Arms," *IEEE Transactions on Robotics and Automation*, Vol. 9, No. 5, 1993, pp. 571–580.

[13]Wee, L.-B., and Walker, M. W., "On the Dynamics of Contact Between Space Robots and Configuration Control for Impact Minimization," *IEEE Transactions on Robotics and Automation*, Vol. 9, No. 5, 1993, pp. 581–591.

[14]Lee, S., and Lee, H. S., "Modeling, Design, and Evaluation of Advanced Teleoperator Control Systems with Short Time Delay," *IEEE Transactions on Robotics and Automation*, Vol. 9, No. 5, 1993, pp. 607–623.

[15]Papadopoulos, E., and Dubowsky, S., "On the Nature of Control Algorithms for Free-Floating Space Manipulators," *IEEE Transactions on Robotics and Automation*, Vol. 7, No. 6, 1991, pp. 750–758.

[16]Spofford, J., and Akin, D., "Redundancy Control of a Free-Flying Telerobot," Space Systems Lab., Massachusetts Inst. of Technology, Cambridge, MA, 1988.

[17]Umetani, Y., and Yoshida, K., "Resolved Motion Rate Control of Space Manipulators with Generalized Jacobian Matrix," *IEEE Transactions on Robotics and Automation*, Vol. 5, No. 3, 1989, pp. 303–314.

[18]Vafa, Z., and Dubowsky, S., "On the Dynamics of Manipulator in Space Using the Virtual Manipulator Approach," *Proceedings of IEEE International Conference on Robotics and Automation* (Raleigh, NC), Vol. 1, 1987, pp. 579–585.

[19]Mukherjee, R., and Nakamura, Y., "Formulation and Efficient Computation of Inverse Dynamics of Space Robots," *IEEE Transactions on Robotics and Automation*, Vol. 8, No. 3, 1992, pp. 400–406.

[20]Nenchev, D., Umetani, Y., and Yoshida, K., "Analysis of a Redundant Free-Flying Spacecraft/Manipulator Systems," *IEEE Transactions on Robotics and Automation*, Vol. 8, No. 1, 1992, pp. 1–6.

[21]Ehrenwald, L., Guelman, M., and Van Woerkom, P. T. L. M., "Dynamics and Control of a Free Flying Two-Armed Robot in Space," 32nd Israel Annual Conf. on Aeronautics and Astronautics, Tel-Aviv, Feb. 1992.

[22]Guelman, M., "Dynamics and Control of a Spacecraft Based Manipulator," National Aerospace Lab. (NLR), TR 87 047 L, Amsterdam, The Netherlands, Feb. 1987.

[23]Lindberg, R. E., Longman, R. W., and Zedd, M. F., "Kinematics and Reaction Moment Compensation for a Spaceborne Elbow Manipulator," AIAA Paper 86-0250, Jan. 1986.

[24]Longman, R. W., "Attitude Tumbling Due to Flexibility in Satellite Mounted Robots," AIAA Paper 88-4096, Jan. 1988.

[25]Longman, R. W., "The Kinetics and Workspace of a Robot Mounted on a Satellite That Is Free to Rotate and Translate," AIAA Paper 88-4097, Jan. 1988.

[26]Van Woerkom, P. T. L. M., and Guelman, M., "Dynamics Modeling, Simulation, and Control of a Spacecraft/Manipulator System," *Proceedings of the First European In-Orbit Operations Technology Symposium*, ESA SP-272, European Space Agency, Darmstadt, Germany, 1987, pp. 439–448.

[27]Craig, J. J., Hsu, P., and Sastry, S. S., "Adaptive Control of Mechanical Manipulators," *International Journal of Robotics Research*, Vol. 6, No. 2, 1987, pp. 16–28.

[28]Slotine, J.-J. E., and Li, W., "On the Adaptive Control of Robot Manipulators," *International Journal of Robotics Research*, Vol. 6, No. 3, 1987, pp. 49–59.

[29]Feng, G., and Palaniswami, M., "Adaptive Control of Robot Manipulators in Task Space," *IEEE Transactions on Automatic Control*, Vol. 38, No. 1, 1993, pp. 100–104.

[30]Spong, M. W., and Ortega, R., "On Adaptive Inverse Dynamics Control of Rigid Robots," *IEEE Transactions on Automatic Control*, Vol. 35, No. 1, 1990, pp. 92–95.

[31]Middleton, R. H., and Goodwin, G. C., "Adaptive Computed Torque Control for Rigid Link Manipulators," *Proceedings of the IEEE Conference on Decision and Control*, Inst. of Electrical and Electronics Engineers, New York, 1987, pp. 68–73.

[32]Gourdeau, R., and Schwartz, H. M., "Adaptive Control of Robotic Manipulators Using an Extended Kalman Filter," *Journal of Dynamic Systems, Measurement and Control*, Vol. 115, March 1993, pp. 203–208.

[33]Kanade, T., and Khosla, P. K., "An Algorithm to Estimate Manipulator Dynamics Parameters," *International Journal of Robotics and Automation*, Vol. 2, No. 3, 1987, pp. 127–135.

[34]Xu, Y., Shum, H.-Y., Kanade, T., and Lee, J.-J., "Parametrization and Adaptive Control of Space Robot Systems," *IEEE Transactions on Aerospace and Electronic Systems*, Vol. 30, No. 2, 1994, pp. 435–451.

[35]Slotine, J.-J. E., and Li, W., "Adaptive Manipulator Control: A Case Study," *IEEE Transactions on Automatic Control*, Vol. 33, No. 11, 1988, pp. 995–1003.

[36]Walker, M. W., and Wee, L.-B., "Adaptive Control of Space-Based Robot Manipulators," *IEEE Transactions on Robotics and Automation*, Vol. 7, No. 6, 1991, pp. 828–835.

[37]Yuan, J., and Stepanenko, Y., "Robust Adaptive Control of Robotic Manipulators Without the Regressor Matrix," *International Journal of Adaptive Control and Signal Processing*, Vol. 6, March 1992, pp. 111–126.

[38]Sadegh, N., and Horowitz, R., "An Exponentially Stable Adaptive Control Law for Robot Manipulators," *IEEE Transactions on Robotics and Automation*, Vol. 6, No. 4, 1990, pp. 491–496.

[39]Craig, J. J., *Adaptive Control of Mechanical Manipulators*, Addison–Wesley, Reading, MA, 1988, pp. 44–47, 49–84, 123–133.

[40]Ortega, R., and Spong, M. W., "Adaptive Motion Control of Rigid Robots: A Tutorial," *Automatica*, Vol. 25, No. 6, 1989, pp. 877–888.

[41]Dubowsky, S., and DesForges, D. T., "The Application of Model-Referenced Adaptive Control to Robotic Manipulators," *Journal of Dynamic Systems, Measurement and Control*, Vol. 101, Sept. 1979, pp. 193–200.

[42]Van Woerkom, P. T. L. M., Guelman, M., and Ehrenwald, L., "Integrated Adaptive Control for Space Manipulators," *Acta Astronautica*, Vol. 38, No. 3, 1996, pp. 161–174.

[43]Gelb, A. (ed.), *Applied Optimal Estimation*, MIT Press, Cambridge, MA, 1974, pp. 102–143, 182–200.

[44]Goodwin, G. C., and Sin, K. S., *Adaptive Filtering, Prediction and Control*, Prentice–Hall, Englewood Cliffs, NJ, 1984, pp. 47–100.

[45]Narendra, K. S., and Annaswamy, A. M., *Stable Adaptive Systems*, Prentice–Hall, Englewood Cliffs, NJ, 1989, pp. 85, 86.